Asymmetrical Molecular Junctions with Different Alligator Clips

Rupan Preet Kaur, Ravinder Singh Sawhney, and Derick Engles
Department of Electronics Technology, Guru Nanak Dev University, Amritsar, India
Email: bhullar.rupan@gmail.com, sawhney_gndu@hotmail.com, derickengles@yahoo.com

***Abstract*—This paper describes different molecular junctions with different alligator clips connected to gold electrodes at nanometre-scale. Our objective was to determine the charge transport characteristics of these junctions and determine the optimum alligator clip pair. We scrutinised anthracenedithiol (ADT), anthracenediamine (ADA) and anthracenethiolamine (ATA) and computed their conductance parameters through our simulations via Semi Emperical Extended Huckel Theory Approach. We aimed at finding that whether symmetrical (same alligator clips at each side) or asymmetrical (different alligator clips at each side) is the optimised approach to connect the anthracene molecule with gold electrodes and found that different alligator clips i.e. thiol and amine exhibited more conduction than that of same clip pair i.e. ADT and ADA. We further examined the effect of changing alligator clips positions from para to meta and found varied quantum interference effects. Peak to valley current ratios (PVR) for ADT was found to be maximum as 7.05 whereas meta ATA exhibited lowest peak to valley current ratio of 1.44.**

***Index Terms*—thermoelectric, nano-junction, tunnelling, quantization, alligator clips, HOMO, LUMO, fermi level**

I. Introduction

Although molecular electronics has been proposed as an alternative to silicon in post-CMOS devices, molecules with unique functions may have applications that are complementary to the silicon-based microelectronics. Many molecules with wonderful electronic, optical, magnetic, thermoelectric, electromechanical and molecular recognition properties have been identified and synthesized in chemistry labs [1]. Hence, electron transport through molecular devices connected to metallic electrodes at nanoscale is the basis of future of electronics technology. The metal-SC nanojunction was treated theoretically by Landman et al. (2000) who studied the nanocontacts formed between Si-nanowires and Al nanoelectrodes. These authors predicted the induction of sub-gap states near the Si-Al interface, which rapidly decay into the Si, and the development of relatively large Schottky barrier [2]. Only few experiments, however, have been realized which target current through a single molecule while the connection to both electrodes is symmetrically realized by a well defined chemical bond, which allows mechanical stability of the junction even at room temperature [3], [4]. The charge is transferred under the bias voltage and current-voltage (I-V) characteristics are measured experimentally [5]. The transport properties of such structures are dominated by some effects of quantum origin, such as: tunnelling, quantization of molecular energy levels and discreteness of electron charge and spin [6]-[13]. Since the tunnelling decay constant of π-conjugated molecules (0.2Å-1) is smaller typically by 1 order of magnitude than that observed for σ-bonded ones (1.0Å-1), we can say that π-Conjugated molecules are expected to form high conductive wires [14]. The small energy gap between the lowest unoccupied molecular orbital (LUMO) and the highest occupied molecular orbital (HOMO) is favourable for injection and tunnelling of charged carriers.

The potential ability of π-conjugated molecules as conductive wires is evident from the studies on photo-induced and electrochemical charge transfer rate through molecules [15]-[18]. Numerous experimental results and contributions on charge transport through molecular junctions [19], [20] suggest that the transport characteristics are controlled by the intrinsic properties of the molecules, the contacts ("alligator clips"), and the metal leads. These include the molecular length, conformation, the gap between HOMO and LUMO, the alignment of this gap to the metal Fermi level, temperature, mechanical stress and the metal-molecule coordination geometry. In this research, we have concentrated on the contacts or alligator clips and by making certain changes with the anthracene molecule, the conduction properties were scrutinised. In the first two epochs, we considered anthracene molecule terminated by thiol group and amine group at each side respectively and the symmetry was preserved whereas in third epoch, we considered one thiol clip and other amine clip at two different sides of anthracene molecule connecting to gold electrodes i.e. Asymmetry was obtained in anthracenethiolamine (ATA) and symmetrical molecules anthracendithiol (ADT) and anthracenediamine (ADA) were taken into consideration in our study. We computed their charge transport characteristics which are reported below. Further, some theoretical aspects of interference phenomena in anthracene molecule connecting two gold electrodes by thiol (–SH) and amine (NH_2) endgroups by changing their positions from para to meta were also

Manuscript received July 15, 2013; revised October 24, 2013

doi: 10.12720/ijmse.1.2.112-117

studied. These end groups, since hydrogen atom is lost in the chemisorption process, ensured readily attachment to metal surfaces [21]. Anthracene molecule between two electrodes acts as an "electronic interferometer". Interference reveals the wave nature of the electrons passing from the source to drain through the molecule. Here the variation of interference conditions was achieved by changing the connection between anthracene molecule and electrodes.

II. Modeling and Simulation

We have considered our modeling and simulation of the electron transport through anthracene stringed to two semi-infinite gold electrodes having (1, 1, 1) configuration using different alligator clips: A) Anthracenedithiol (ADT) B) Anthracenedamine (ADA) C) Anthracenethiolamine (ATA).

For our modelling, we employed semi-empirical extended huckel theory (EHT) for the purpose of tight binding as well as time constraint. The molecular junctions are shown in Fig. 1 which shows anthracene molecule stretched between two gold electrodes with different endgroups. In Fig. 1 c), anthracenethiolamine (ATA) is shown in which we had sulphur at left side bounding anthracene to left electrodes and amine group at right side. Both theses alligator clips connected anthracene to electrodes via para positions as para positions are linearly conjugated, whereas the meta position is cross-conjugated [22]. The meta position of thiol and amine endgroups connecting anthracene to gold electrodes is shown in Fig. 2. Gold electrodes have been generally used in single molecule junctions because of their stability in air. The quantum mechanical First-principle transport calculations for a two-probe system were performed using Atomistic Tool Kit 12.2.0 [23] and its graphical interface employing semi-empirical Extended Huckel Device Theory. The aim of this work is to compute the charge transport characteristics of ADT, ADA and ATA and by comparing them, finding the optimised alligator clip pair for anthracene molecule.

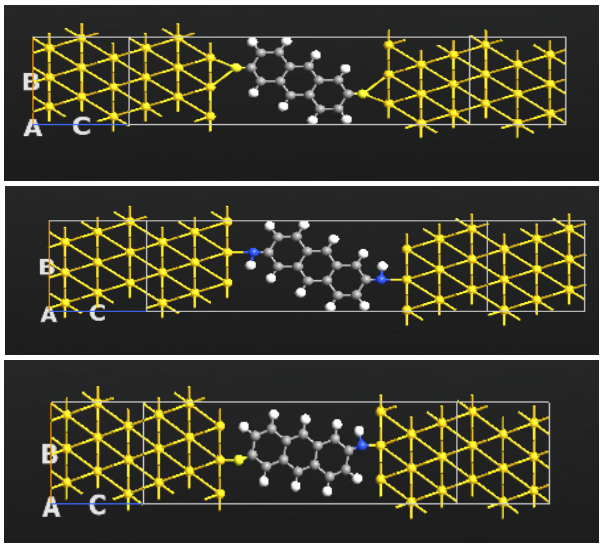

Figure 1. Molecular junctions comprising: A) ADT B) ADA C) ATA in para position

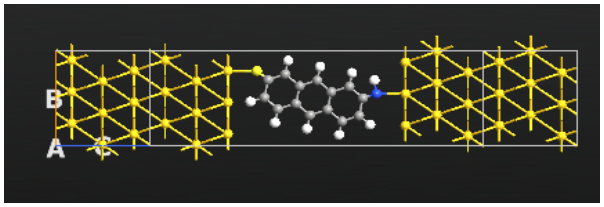

Figure 2. Anthracenethiolamine (ATA) in meta position

III. Results and Discussions

We have modelled anthracene molecule with different end group anchors - Sulphur at one end and amine group at other end, called anthracenethiolamine (ATA) sandwiched between two semi-infinite gold electrodes (1, 1, 1) orientation. We simulated I-V curves, transmission spectra and conductance curves at various applied bias ranging from -1.2V to 1.2V. Further, we simulated the above said transport characteristics of anthracenedithiol (ADT) and anthracenediamine (ADA) to compare their best possible conduction and conclude the optimum alligator clip pair.

A. I-V Curve

The current can be calculated by firstly calculating transmission function given by [24]:

$$T(E,V) = \frac{1}{\Omega}\int \pi \; dK \; Tk.(E,V) \qquad (1)$$

The transmission functions at k, Tk (E) are expressed in terms of Green's functions as [25], [26]:

$$T_K(E,V) = T_R\,[\Gamma' 1k\,(E,V)\;GMk\,(E,V)\;\Gamma'\,2\,k\,(E,V)\;GMk'\,(E,V)\,] \qquad (2)$$

Expression (2) describes the broadening of molecular energy levels due to the coupling to electrodes. Then I-V characteristics can be computed by Landauer-Buttiker formulism [27] given by:

$$I(V) = 2e/h.\int T(E)\,[f(E-\mu_S) - f(E-\mu_D)]dE \qquad (3)$$

The values of currents at different bias voltages from -1.2 to 1.2V were computed through the simulations that are reported in Table I and shown in Fig. 2.

TABLE I: Current Versus Bias Voltage of ATA

Voltage(v)	Current(nA)
-1.2	-464
-0.8	-455
-0.4	-441
0	0
0.4	1412
0.8	5122
1.2	5379

From Fig. 3, we observed that the current was dormant during negative bias region; increased during positive bias and attained its maximum peak value at highest bias considered in this simulation i.e. 5379nA at 1.2V peak voltage whereas lowest or valley current was found to be -464nA at valley voltage -1.2V.

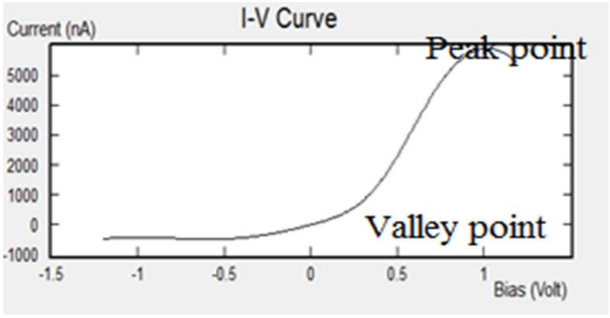

Figure 3. I-V curve of ATA

At low bias, the current can be represented as [28]:

$$I \propto V \exp\left(-\frac{2d\sqrt{2m\varphi}}{h}\right) \quad (4)$$

where φ is the barrier height, d is the molecular length, m is the electron effective mass and h is the Planck's constant. The barrier height corresponds to the difference between Fermi level of gold electrodes and HOMO (highest occupied molecular orbital) energy level, leading to different currents at different bias voltages. Hence, this increase in current reported above is because of different barrier height levels at different bias, lowest bias (-1.2V) corresponds to highest barrier height whereas highest bias (1.2V) corresponds to lowest barrier height and hence maximum electron jumps and hence maximum current. Then the I-V curves of ADT and ADA were compared with that of ATA and the results are reported in Fig. 4.

From Fig. 4, we observed that ADT exhibited peak current of 1411nA at 1.2V peak voltage and valley current -8461nA at -1.2V valley voltage whereas ADA exhibited lowest negligible peak current of 6nA at same peak voltage 1.2V and least current -9.8nA at voltage -1.2V. ATA attained highest value of 5379nA, hence contributing maximum conduction. Since, ADA exhibited almost constant current as shown in Fig. 4, hence, the molecular junction comprising ADA can be used as current-limiting or current regulating diode and for charging secondary batteries. The increasing order of current exhibited by these molecular junctions was: ADA<ADT<ATA.

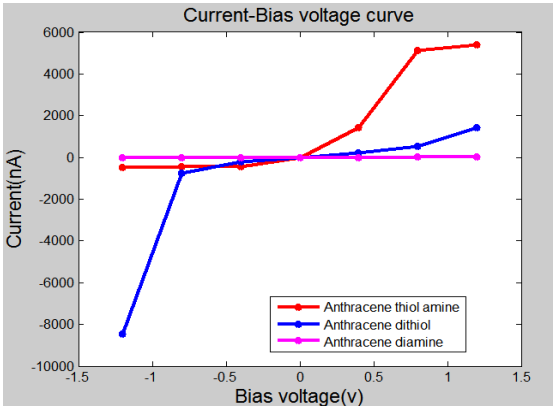

Figure 4. I-V curve comparison of ADT, ADA and ATA

B. Conductance

The quantized conductance of the molecule can be given by the relation:

$$G_0 = N.e^2/h \quad (5)$$

Here e and h are electron charge and plank's constant respectively, while N depends upon the spin. The quantized conductance G0 is the conductance at zero bias and this value works out to be 77.5 μS. The total transmission coefficient is also a function of conductance at any bias voltage and is given by [29]:

$$G = G_0 . T(E_f) \quad (6)$$

where $T(E_F)$ is the transmission coefficient at Fermi energy. The conductance values of ATS were computed corresponding to the bias voltages and reported as shown in Table II.

TABLE II. CONDUCTANCE-BIAS VOLTAGE OF ATA

Bias voltage(V)	Conductance(nS)
-1.2	488.9
-0.8	489.9
-0.4	516
0	977
0.4	11710
0.8	747
1.2	962

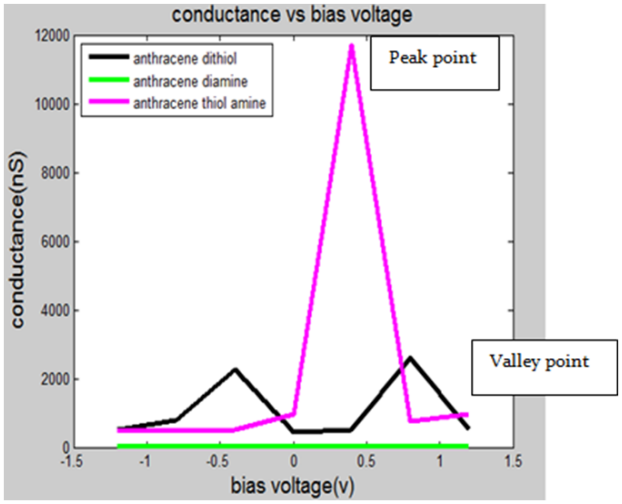

Figure 5. Conductance-voltage comparison of ADT, ADA and ATA

From Table II and Fig. 5, we again observed that because the current remained dormant during negative bias, hence conductance also remained almost constant during negative bias but as the bias crossed 0V, due to decrease in barrier height, conductance increased linearly and attained maximum conductance 11710nS or $0.15G_0$ at 0.4V and finally showed negative differential conductance behaviour at high bias voltages taken into consideration. From Fig. 5, the region between peak point and valley point is called negative differential

region. The currents at both ON (high conduction state) to OFF (low conduction state) are space-charge limited and attributed to the electron traps at the interface between the Au electrodes and the molecule. The current initially increased with the positive bias as electrons tunnel through the junction barrier because the conduction band is aligned with the valence band. As voltage increased further, the conduction and valence bands became misaligned and the conductance dropped, resulting in NDR. This mechanism of conduction is called inter-band tunneling [1]. The curve shown in Fig. 5 comprises the region where current increased to negative conductance peak and then showed negative conductance effect. Negative conductance characteristic peak is due to quantum mechanical tunnelling involving the dual particle-wave nature of electrons. The depletion region is thin enough compared with the equivalent wavelength of the electron that they can tunnel through. With increasing voltage, tunnelling begins; the levels overlap; current increases, up to a point. As current increases further, the energy levels overlap less; current decreases with increasing voltage. Moreover, we observed that anthracenediamine (ADA) showed negligible conductance, whereas anthracenedithiol (ADT) showed two triangular waveforms with two peaks at -0.4V and 0.8V and remained negligible at other points. ATA showed maximum conduction of $0.15G_0$ at 0.4V and remained low at other voltages. Here again, we can say that ADT and ATA exhibited negative differential conductance where we found -0.4V and 0.8V ON states for ADT and OFF at other voltages whereas ATA showed ON state at 0.4V and remained OFF at other bias voltages.

C. *Transmission Spectra*

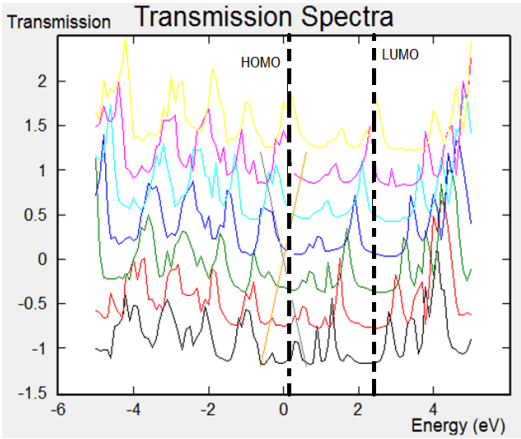

Figure 6. Transmission spectra of para ATA

The transmission spectrum shows the coupling between the electrodes and the molecule that leads to overlapping of the hybridized orbitals and a change in HOMO-LUMO gaps. The stronger the coupling, more the orbitals are broadened and lesser will be the energy gap to jump for electrons. Sharp peaks in the spectrum show maximum transmissions (smaller HOMO-LUMO gap) whereas flatness shows minimum transmissions (greater HOM-LUMO gap) [30]. Fig. 6 and Fig. 7 show the transmission spectra of para and meta ATA where we observed peaks and flatness that correspond to maximum and no transmissions respectively. Transmission spectra of Para ATA showed HOMO and LUMO levels around 0 eV and 2.2eV energy respectively whereas that of meta exhibited -2eV and 2.2eV respectively. Since, electrons need to gain energy to cross this energy gap and contributing to conduction, it implied that electrons needed smaller work function in para ATA whereas larger work function in meta ATA in order to overcome the forbidden region, hence further confirming our conclusion that para ATA is more conductive than meta ATA.

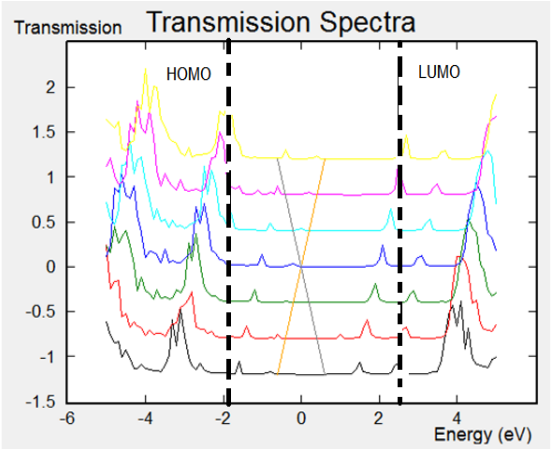

Figure 7. Transmission spectra of meta ATA

Fig. 8 also shows the resultant spectra of para ATA and meta ATA so formed which shows T (E) with different energy range (E_f -E). Para ATA and meta ATA from Fig. 8 shows maximum T (E) of 5 units and 3.5 units respectively. Hence, we concluded para ATA to be more conductive as compared to meta where comparatively lesser transmissions took place in contrast to former case. From Fig. 9, we observed that meta ATA exhibited comparatively lesser current during negative bias region whereas greater current during positive bias than its para counterpart. Fig. 9 shows conductance comparison of para and meta ATA where we observed that meta ATA exhibited more conductance except the peak value.

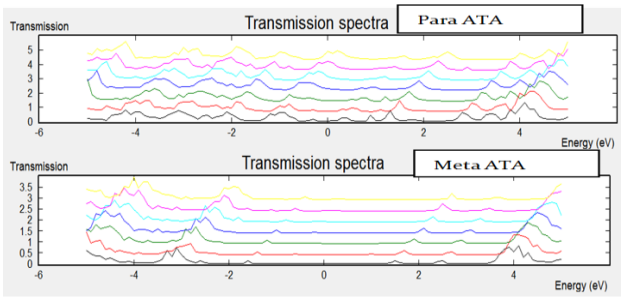

Figure 8. Transmission spectra of Para ATA and meta ATA where we found higher T (E) and more peaks in Para ATA whereas lower T (E) and comparatively, flatness in meta ATA.

Para ATA corresponds to peak of 0.15G0 at 0.4V whereas meta ATA corresponds to $0.097G_0$ at 0V.

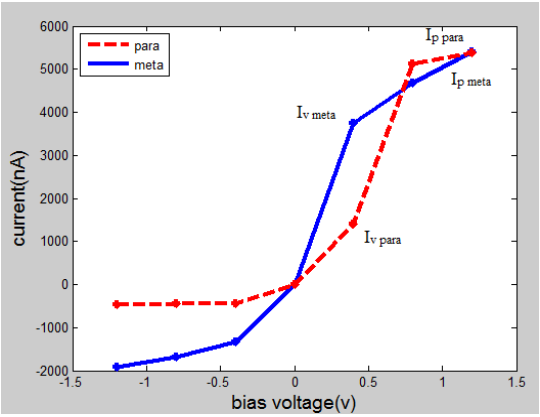

Figure 9. I-V curve comparison of para and meta ATA

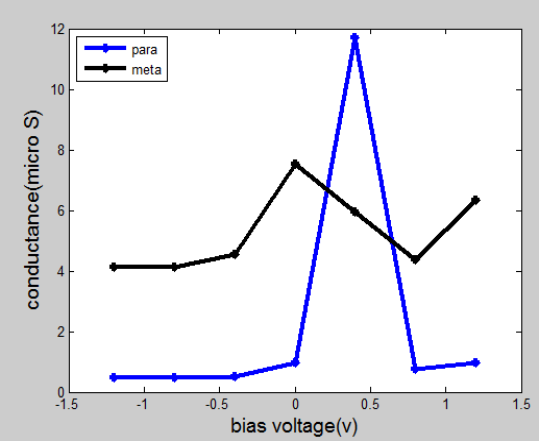

Figure 10. Conductance versus voltage comparison of para and meta ATA

Higher current values during positive bias and higher conductance of meta ATA compared to para ATA was reported in above results. This was on account of change in quantum interference and obvious changes in transmission function with change in positions of alligator clips. It manifests itself as shifts in the resonance peaks and in reduction of their height. Well-separated energy levels give rise to distinct peaks in the spectrum as shown in Fig. 7 and Fig. 10. Large resonant peaks were observed during positive bias of meta ATA as compared to that of para ATA. Large resonant peaks correspond to constructive quantum interference whereas reduced peaks indicate destructive quantum interference. We conclude here that meta ATA exhibited constructive quantum interference because of which it showed more current and conductance as compared to para ATA where destructive quantum interference took place.

D. Peak Valley Current Ratio(PVCR)

As a forward bias voltage is applied, an electric field is created that causes electrons to move from the emitter to the collector by tunnelling through the scattering states within the quantum well. These quasi bound energy states are the energy states that allow for electrons to tunnel through creating a current. As more and more electrons in the emitter have the same energy as the quasi-bound state, more electrons are able to tunnel through the well, resulting in an increase in the current as the applied voltage is increased. When the electric field increases to the point where the energy level of the electrons in the emitter coincides with the energy level of the quasi-bound state of the well, the current reaches a maximum. As the applied voltage continues to increase, more and more electrons are gaining too much energy to tunnel through the well and the current is decreased. After a certain applied voltage, current begins to rise again because of substantial thermionic emission where the electrons can tunnel through the non-resonant energy levels of the well [31]. This process produces a minimum "valley" current that can also be called as the leakage current. High PVR means sharper the I-V curve in negative differential resistance region. From the I-V curves, peak and valley currents of all the molecular junctions comprising ADT, ADA and ATA under study are reported in Table 3 and shown in Fig. 11. The ratio of peak current to valley current was plotted in Fig. 11 where we observed that ADT exhibited highest I_p/I_v whereas meta ATA exhibited lowest I_p/I_v. The increasing order of I_p/I_v was found to be: Meta ATA <ADA<Para ATA<ADT.

TABLE III: PEAK CURRENT, VALLEY CURRENT AND PVCR

Molecule	Peak current (I_p) nA	Valley current (I_v) nA	I_p/I_v
ADT	1411	200	7.05
ADA	6	3.98	1.51
ATA Para	5379	1412	3.81
ATA Meta	5414	3752	1.44

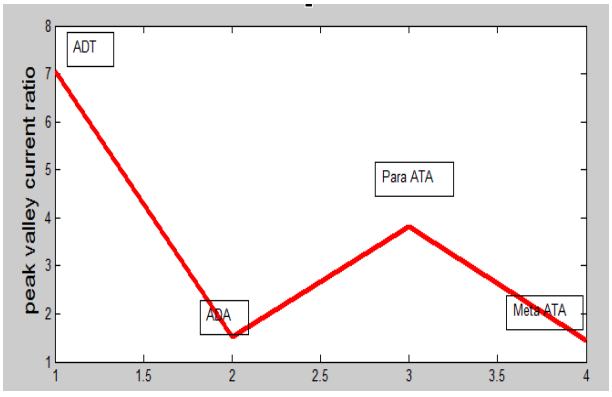

Figure 11. I_p/I_v comparisons of ADT, ADA, ATA

IV. CONCLUSION

We have simulated molecular junction comprising ATA in para position between two gold electrodes for charge transport characteristics-current, conductance and transmission spectra and further compared these parameters with that of ADT and ADA. We found that different alligator clips ATA (Asymmetrical junction) exhibited highest conduction than that of same clips (Symmetrical junction) i.e. ADT and ADA. PVR was found to be highest for ADT whereas lowest for meta ATA. A minimum PVCR of about 3 is needed for typical circuit applications. Low current density tunnel diodes

are suitable for low-power memory applications, and high current density tunnel diodes are needed for high-speed digital/mixed-signal applications. Also, we observed the variation in quantum interference by varying the connections of anthracene and electrodes by switching the anchor positions from para to meta in ATA. We found that meta and para ATA exhibited constructive and destructive quantum interference respectively. The results through this research can be very helpful in proliferating the conductance by varying the symmetry of molecular junctions with different alligator clips. The most popular alligator clip pair 'thiol-thiol' can now be substituted by a number of different optimum clip pairs. Here, we took 'thiol-amine' pair and it exhibited higher current, conductance and more transmissions as compared to that same monotonous pair 'thiol-thiol' which is often considered by researchers. This study has opened a gateway to find the optimum alligator clip pair which can increase the conduction further than that of junctions comprising thiol as alligator clips. This study can further be extended to cyanide, isocyanide, fullerene endgroups which can further aggrandise the conduction that we are getting via molecular junctions having symmetrical clips that we are getting via molecular junctions having symmetrical clips.

ACKNOWLDEGMENT

The authors acknowledge the support by C.S.I.R. under Grant No. 22(0519)10/EMR-II.

REFERENCES

[1] N. J. TAO, "Electron transport in molecular junctions," *Nature Nanotechnology*, vol. 1, pp. 173-181, 2006.
[2] H. Woldeghebriel, "Electronic structure of cdse nanowires terminated with gold electrodes," *Momona Ethiopian Journal of Science*, vol. 3, no. 1, pp. 5-19, 2011.
[3] M. A. Reed, C. Zhou, C. J. Muller, T. P. Burgin, and J. M. Tour, "Conductance of a molecular junction," *Science*, vol. 278, pp. 252-254, 1997.
[4] C. Kergueris, *et al*., "Electron transport through a metal-molecule-metal junction," *Phys. Rev. B*, vol. 59, 1999.
[5] M. A. Reed, "Molecular-Scale Electronics," *Proceedings of the IEEE*, vol. 87, no. 4, Apr. 1999.
[6] P. Sautet and C. Joachim, "Electronic interference produced by a benzene embedded in a polyacetylene chain," *Chem. Phys. Lett.*, vol. 153, no. 6, pp. 511-516, 1988.
[7] V. Marvaud, J. P. Launay, and C. Joachim, "Electron transfer through 2, 7, 9, 10-tetraazaphenanthrene: A quantum "interference" effect?" *Chem. Phys*, vol. 177, no. 1, pp. 23-30, 1993.
[8] M. N. Paddon-Row and K. D. Jordan, "Analysis of the distance dependence and magnitude of the. pi.+,. pi.- and. pi.+*,. pi.-* splittings in a series of diethynyl [n] staffanes: an ab initio molecular orbital study," *J. Am. Chem. Soc*., vol. 115, no. 7, pp. 2952-2960, 1993.
[9] E. Emberly and G. Kirczenow, "Antiresonances in molecular wires," *J. Phys.: Condens. Matter*, vol. 11, 1999.
[10] M. Magoga and C. Joachim, "Conductance of molecular wires connected or bonded in parallel," *Phys. Rev. B*, vol. 59, no. 24, 1999.
[11] C. Untiedt, G. R. Bollinger, S. Vieira, and N. Agrait, "Quantum interference in atomic-sized point contacts," *Phys. Rev. B*, vol. 62, no. 15, 2000.
[12] R. Baer and D. Neuhauser, "Phase coherent electronics: A molecular switch based on quantum interference," *J. Am. Chem. Soc*., vol. 124, no. 16, pp. 4200-4201, 2002.
[13] R. Baer and D. Neuhauser, "Anti-coherence based molecular electronics: XOR-gate response," *Chem. Phys*., vol. 281, no. 2, pp. 353-362, 2002.
[14] A. Salomon, D. Cohen, S. Lindsay, J. Tomfohr, V. B. Engelkes, and C. D. Frisbie, "Comparison of electronic transport measurements on organic molecules," *Advanced Materials*, vol. 15, no. 22, pp. 1881-1890, 2003.
[15] C. Joachim and M. A. Ratner, "Molecular wires: guiding the super-exchange interactions between two electrodes," *Nanotechnology*, vol. 15, no. 8, pp. 1065-1075, 2004.
[16] T. Otsubo, Y. Aso, and K. Takimiya, "Functional oligothiophenes as advanced molecular electronic materials," *J. Mater. Chem.*, vol. 12, pp. 2565-2575, 2002.
[17] D. Holten, D. F. Bocian, and J. S. Lindsey, "Probing electronic communication in covalently linked multiporphyrin arrays," *J. S. Acc. Chem. Res*., vol. 35, no. 1, pp. 57-69, 2002.
[18] H. D. Sikes, *et al.*, "Rapid electron tunneling through oligophenylenevinylene bridges," *Science*, vol. 291, no. 5508, pp. 1519-1523, 2001.
[19] S. B. Sachs, S. P. Dudek, *et al*., "Rates of interfacial electron transfer through π-conjugated spacers," *J. Am. Chem. Soc.*, vol. 119, pp. 10563-10564, 1997.
[20] A. Nitzan and M. A. Ratner, "Electron transport in molecular wire junctions," *Science*, vol. 300, no. 5624, pp. 1384-1389, 2003.
[21] A. Pecchia and A. D. Carlo, "Atomistic theory of transport in organic and inorganic nanostructures," *Rep. Prog. Phys.*, vol. 67, no. 8, pp. 1497-1561, 2004.
[22] H. Sellers, A. Ulman, Y. Shnidman, and J. E. Eilers, "Structure and binding of alkanethiolates on gold and silver surfaces," *J. Am. Chem. Soc*., vol. 115, no. 21, pp. 9389-9401, 1993.
[23] R. S. Sawhney and D. Engles, "Geometry related quantum interference for stress and conductance of an organic molecule," in *Proc. Nanocon*, 2012, pp. 1219-1224.
[24] *Atomistic Toolkit Manual*, Quantumwise Inc.
[25] Y-H. Kim, S. S. Jang, and W. A. Goddard, "Conformations and charge transport characteristics of biphenyldithiol self-assembled-monolayer molecular electronic devices: A multiscale computational study," *The Journal of Chemical Physics*, vol. 122, no. 24, 2005.
[26] S. Datta, W. Tian, S. Hong, R. Reifenberger, J. I. Henderson, and C. P. Kubiak, "Current-voltage characteristics of self-assembled monolayers by scanning tunneling microscopy," *Phys. Rev. Lett*., vol. 79, no. 13, 1997.
[27] P. Damle, A. W. Ghosh, and S. Datta, "Unified description of molecular conduction: From molecules to metallic wires," *Phys. Rev. B*, vol. 64, no. 20, 2001.
[28] S. Datta, *Electronic Transport in Mesoscopic Systems*, UK: Cambridge University Press, 1995.
[29] Y. Z. Wu, "Length-Dependent Conductance of Conjugated Molecular Junctions," S1951319.
[30] Ravinder Singh Sawhney and Derick Engles, "Predicting optimal anchoring group for quantum transport through anthracene," in *Proc. ETMN*, BITS, India, 2013, pp. 215-216.
[31] R. P. Kaur, R. S. Sawhney, R. Kaur, and D. Engles, "Single-molecule junctions based on selenol-terminated anchor-a promising candidate for electron transport," in *Proc. International Conference on Advanced Nanomaterials and Emerging Engineering Technologies*, 2013, pp. 431-435.
[32] J. Ling, "Resonant tunneling diodes: Theory of operation and applications," *Appl. Phy. Lett.*, vol. 73, 1998.

Rupan Preet Kaur, Research Scholar in the Department of Electronics Technology, G.N.D.U, Amritsar, is doing her research work in the field of modeling and simulation of electron transport at nanometre scale towards the fabrication of Molecular electronic devices.

Ravinder Singh Sawhney, professor in the Department of Electronics Technology, Guru Nanak Dev University, Amritsar. He has to his credit more than 80 publications in various international journals as well as international and national conference proceedings.

Derick Engles, professor in the Department of Electronics Technology, Guru Nanak Dev University, Amritsar. He has to his credit more than 160 publications in various international journals as well as international and national conference proceedings.

